



HAL
open science

New force field for GCMC simulations of D₂/H₂ quantum sieving in pure silica zeolites

Bastien Radola, Maxence Giraudet, Igor Bezverkhyy, Jean Marc Simon, J. Marcos Salazar, Mathieu Macaud, Jean Pierre Bellat

► **To cite this version:**

Bastien Radola, Maxence Giraudet, Igor Bezverkhyy, Jean Marc Simon, J. Marcos Salazar, et al.. New force field for GCMC simulations of D₂/H₂ quantum sieving in pure silica zeolites. *Physical Chemistry Chemical Physics*, 2020, 22 (42), pp.24561-24571. 10.1039/D0CP03871G . hal-03006840

HAL Id: hal-03006840

<https://hal.science/hal-03006840>

Submitted on 30 Nov 2020

HAL is a multi-disciplinary open access archive for the deposit and dissemination of scientific research documents, whether they are published or not. The documents may come from teaching and research institutions in France or abroad, or from public or private research centers.

L'archive ouverte pluridisciplinaire **HAL**, est destinée au dépôt et à la diffusion de documents scientifiques de niveau recherche, publiés ou non, émanant des établissements d'enseignement et de recherche français ou étrangers, des laboratoires publics ou privés.

New force field for GCMC simulation of D₂/H₂ quantum sieving in pure silica zeolites

Bastien Radola^a, Maxence Giraudet^{a,b}, Igor Bezverkhyy^a, Jean Marc Simon^a, José-Marcos Salazar^a, Mathieu Macaud^b and Jean Pierre Bellat^{a*}

^a Laboratoire Interdisciplinaire Carnot de Bourgogne, UMR 6303 CNRS-Université de Bourgogne Franche-Comté, BP 47870, 21078 Dijon Cedex, France

^b CEA, DAM, VALDUC, F-21120 Is-sur-Tille, France

* Corresponding author: jean-pierre.bellat@u-bourgogne.fr

Abstract:

We report a study on adsorption and coadsorption of H₂ and D₂ in FAU, MFI and CHA pure silica zeolites having different pore size and shape. Adsorption capacities, selectivities, enthalpies and entropies are determined by combining experiments and GCMC simulations. We show that the force fields available in the literature cannot predict the adsorption equilibria below 77 K with sufficient accuracy. Here we propose a new force field adjusted by using our experimental data obtained for pure silica MFI zeolite at 65 K and 77 K. With this new force field, it is possible to predict adsorption and coadsorption equilibria on the three zeolite structures in a temperature range between 47 and 77 K with satisfactory precision. We corroborate that the step appearing on the single adsorption isotherms in CHA is the result of a molecular rearrangement of the adsorbed phase due to the apparition of a new adsorption site characterized by weaker interactions of H₂ with the adsorbent. We conclude that the quantum sieving of H₂ and D₂ does not depend only on the pore size but also on the pore shape, in particular, at high loading when the confinement effects become important.

Introduction

Over the last two decades, the interest in adsorption of hydrogen isotopes at cryogenic temperature has considerably grown in the nuclear industry. The development of new sources of energy based on nuclear fusion (ITER) will use and produce considerable amounts of hydrogen isotopes, which need to be recycled¹. A promising way to recover and separate these isotopes at low cost is physisorption on nanoporous solids at cryogenic temperature (20 – 100 K). One of the driving force for hydrogen isotopes separation is quantum sieving, which appears when the size of the adsorbed molecule (diameter of hydrogen = 0.28 nm) is close to the pore diameter. This phenomenon occurs at low temperature (below 100 K) and makes that heavier molecules are strongly adsorbed and diffuse faster in the nanoporosity. As shown by Beenakker et al.², the smaller the pore radius, the higher the adsorption selectivity for the heaviest isotope is. The separation processes of hydrogen isotopes by adsorption that we are developing are based on the TSA (Temperature Swing Adsorption) technology³. They use a fixed bed adsorbent column working between 30 and 80 K under a pressure close to 10^5 Pa. From a practical point of view, these separation processes require a porous adsorbent with two main properties: (1) the pores have to be small enough to be selective towards the heavier isotope and (2) the adsorption capacity has to be high enough in order to use a reasonable volume of adsorbent and then reduce the size of the adsorbent column under cryogenic temperatures. Therefore, the choice of the adsorbent is based on a subtle balance between adsorption selectivity and adsorption capacity in the operating conditions of separation process.

Numerous potential nanoporous materials able to separate hydrogen isotopes by quantum sieving have been already identified either from adsorption experiments or by molecular

simulations, namely: carbons, zeolites and MOFs. These last, have attracted a particular attention⁴ and have been the subject of a considerable number of studies for estimating their capacity to selectively trap the isotopes. However, it is still difficult to establish a ranking of these adsorbents as a function of their selective adsorption properties towards hydrogen isotopes. The reason is just the lack of accurate experimental data at cryogenic temperatures ($T < 77$ K).

Carbons nanotubes and sieves show interesting D_2/H_2 adsorption selectivities, with values up to 16 at 40 K under 10^5 Pa, when using small pores ($\varnothing < 0.56$ nm)^{5, 6}. It has also been shown that the selectivity greatly depends on the pore geometry. Moreover, significant differences have been observed between slit pores and nanotubes. However their adsorption capacity, around 0.005 mol.g^{-1} under these conditions⁷⁻⁹, are too small for being used in industrial applications.

MOFs are very interesting adsorbents due to their well-defined pore structure which can be tuned by changing the length of the organic chains linking the inorganic units¹⁰. It is also possible to enhance their selective adsorption properties by changing the chemical nature of linkers or metal. In addition, the adsorption of heavier isotopes can be improved by taking advantage of their specific properties like multimodal porosity and framework flexibility. Some MOFs present excellent D_2/H_2 adsorption selectivity with value around 10 at 40 K like for the well-known flexible MIL-53(Al)¹¹. Even the partially fluorinated metal-organic-framework, so-called FMOFCu, can show selectivity values up to 14 at 25 K. This is a result of their capacity to open or close the pores as a function of temperature¹². Unfortunately, the adsorption capacities of these materials are very low: 0.002 mol.g^{-1} for MIL-53 (Al) at 40 K and only $0.0005 \text{ mol.g}^{-1}$ for FMOFCu at 25 K under 10^3 Pa. Like for carbon materials, such adsorption capacities are insufficient for industrial applications. Moreover, the use of organic

material could be hazardous for nuclear applications due to possible isotope exchanges with the matrix. As a consequence, the use of inorganic porous materials is strongly suggested.

Among them, zeolites are promising adsorbents. Owing to their tunable chemical composition and regular porosity, they get both large hydrogen adsorption capacities and interesting adsorption selectivities in favor of deuterium. These properties are strongly dependent on the pore structure and nature of compensation cations¹³⁻¹⁷. For cationic FAU zeolites, D₂/H₂ selectivity can vary from 3 to 6 according to the compensation cation at 77 K and low pressure (a few hPa) corresponding to low loading¹⁸. However, under 10⁵ Pa, which is close to the operating pressure of an adsorption process, the selectivity value is rather low, it does not exceed 2 whatever may be the chemical composition. Although it could seem insufficient in comparison with other materials (MOF, carbon). This is compensated by large adsorption capacities (up to 0.009 mol.g⁻¹ at 77 K under 10⁵ Pa with NaX¹⁸), such that this material is a good candidate for separation processes. Recent Monte-Carlo simulations have shown that non-cationic zeolites could present very high adsorption selectivity¹⁹. In this work, the authors performed a systematic screening of H₂/D₂ mixtures over a large variety of synthesized and hypothetical pure silica zeolites of different topologies. For example, the BCT zeolite shows an adsorption selectivity towards deuterium of around 80 at 40 K under 10⁵ Pa, conditions which are close to those of a separation process. This zeolite is made of a one-dimensional pore system formed by 8-membered oxygen ring (8MR) parallel channels of 0.38 nm diameter. However, the adsorption capacity of BCT is low, around 0.003 mol/g, which is almost ten times lower than for the NaX zeolite at 40K. Such an adsorption capacity is not enough to consider the development of a viable adsorption process with this type of adsorbent. It may be noted that (i) the predictions obtained by molecular simulations have not been yet validated by coadsorption experiments and (ii) the pure silica BCT zeolite is not thermodynamically stable²⁰. Anyhow, this study shows that high silica zeolites having very

small pore composed of 8-membered oxygen rings could be potentially selective adsorbents for the separation of hydrogen isotopes. Henceforth, it appears relevant to study in more details the coadsorption of hydrogen isotopes in pure silica zeolites by combining adsorption experiments and molecular simulation.

Molecular simulations based on Monte Carlo method are a very useful tool for studying the adsorption properties and for the development of a separation process by adsorption²¹. First, as mentioned above, it allows screening of potential selective adsorbents without having to do long and tedious coadsorption experiments. Second, it gives rich information about the coadsorption mechanism at a molecular level, rather difficult to access at cryogenic temperatures. Third, it allows the prediction of coadsorption equilibria of radioactive isotopes like T₂ or HT which can hardly be investigated experimentally. Nonetheless, the choice of the molecular model and the force field must be validated by accurate adsorption and coadsorption experimental data obtained with H₂ and D₂ on well characterized adsorbents. Concerning the zeolites, several molecular simulations of adsorption and diffusion of hydrogen and deuterium are described in the literature²²⁻²⁷. They have been performed with Monte Carlo or Molecular Dynamics methods using different force fields including the Feynman-Hibbs variational approach to take into account quantum effects. Different force fields are used in the literature to describe the adsorption of hydrogen and deuterium in cationic and pure silica zeolites. However, these simulations are compared only with adsorption data of single components measured on few zeolites (NaX, Rho, silicalite-1, Si-LTA) at 77 K or higher temperatures. As far as we know, only few works report a comparison of simulated and experimental adsorption selectivities below 77 K. Probably this is due to the lack of coadsorption experimental data^{22, 28, 29}. Therefore, the achievement of new coadsorption experiments of hydrogen isotopes below 77 K is also an opportunity to test the

force fields presented in the literature and their transferability among zeolitic structures having different pore geometry, but the same chemical composition.

The present work deals with the adsorption and coadsorption of hydrogen and deuterium in three pure silica zeolites: FAU, MFI and CHA. These zeolites differ by their pore geometries (form and aperture) but have the same surface chemistry. Single gas adsorption isotherms and adsorption selectivities of binary H₂ + D₂ mixtures have been measured between 35 and 77 K under 10⁵ Pa. Experimental data are compared with the Grand Canonical Monte-Carlo (GCMC) simulations performed with different force fields to verify if the models describe accurately the zeolite, the gas and their interactions and if necessary to improve them.

Experimental

High silica Zeolites

Three framework types of high silica zeolite were studied: FAU, MFI and CHA. These zeolites can be elaborated at the industrial scale. All were pulverulent and free of binder. Silica FAU was purchased from Degussa (Germany) under the reference DaY. It was obtained by dealumination of the NaY zeolite. Silica MFI was the silicalite-1 elaborated by the company Zephir-Alsace (Mulhouse, France). It was synthesized in fluoride media according to the procedure described by Guth et al.³⁰. Silica CHA was kindly provided by J. Patarin from IS2M laboratory (Mulhouse, France). The zeolite was prepared using the method described by Díaz Cabañas et al.³¹. These materials have been extensively characterized by XRD, FTIR, SEM, NMR and N₂ adsorption in our previous works^{29, 32, 33}. Silica MFI is perfectly crystallized with right morphology and microporosity and without silanol defects.

FAU and CHA have also a good crystallinity though they contain a few mesopores and a few sodium cations are present in FAU.

These silica materials differ by their pore geometries: FAU has quasi-spherical cages ($\text{\O} = 1.1$ nm) with an aperture diameter of 0.74 nm (12MR), MFI has interconnected cylindrical channels of around 0.56 nm diameter (10MR) and CHA has cylindrical shaped cages ($\sim 0.8 \times 1.1$ nm) interconnected with windows of 0.37 nm diameter (8MR). Some physical-chemical characteristics of these silica zeolites are given in Table 1.

Adsorption and coadsorption manometric devices

Adsorption isotherms of single components were measured with a ASAP 2020 Micromeritics sorptometer equipped with a Gifford – McMahon He cryocooler. Adsorption experiments were performed between 47 and 77 K for pressures ranging from 0.1 to 10^5 Pa. Prior to adsorption, the sample (~ 100 mg) was outgassed at 673 K under secondary vacuum overnight. H_2 and D_2 (purity > 99.9 %) gases were purchased from Air Liquide (France) and were additionally dried using zeolite filled cartridges.

Adsorption selectivity of deuterium with respect to hydrogen was measured from coadsorption experiments performed with a home-made manometric device coupled with a quadrupole mass spectrometer OmniStar from Pfeiffer Vacuum. This apparatus and the procedure used have been described in our previous works^{13, 18}. The adsorption temperature was controlled with the cryocooler from Micromeritics. D_2/H_2 selectivities were measured for 25% D_2 + 75% H_2 mixture in the same conditions (temperature, pressure, outgassing...) as for single components. The relative precision of the measurements is of 5 % for the adsorbed amount and 15 % for the adsorption selectivity.

We remind that the adsorption selectivity of D_2 with respect to H_2 is defined by the relation:

$$\alpha_{D_2/H_2} = \frac{x_{D_2} y_{H_2}}{x_{H_2} y_{D_2}} = \frac{N_{D_2}^a P_{H_2}}{N_{H_2}^a P_{D_2}} \quad (1)$$

with x and y the mole fractions in the adsorbed and gas phase, respectively, N^a the adsorbed amount expressed in molecules per unit cell (molec.uc⁻¹) and P the partial pressure at equilibrium.

Molecular simulations

Grand Canonical Monte Carlo (GCMC) simulations were performed with the DL_MONTE package^{34, 35}. The applied conditions were similar to those of the experimental situations. Under these conditions ($47 \leq T \leq 77$ K and $P \leq 10^5$ Pa) the gas can be considered as ideal and, in this case, the fugacity is equivalent to the pressure. For convenience we fixed the fugacity instead of the chemical potential, μ , in the GCMC input data.

The quantum effects arising at cryogenic temperature ($T < 100$ K) with hydrogen isotopes are included by using the Feynman-Hibbs approach^{36, 37}:

$$V_{FH}(r_{ij}) = \left(\frac{6M_{ij}}{\pi\beta\hbar^2} \right)^{\frac{3}{2}} \iiint_{-\infty}^{+\infty} V(|r_{ij} + u|) e^{-u^2 \left(\frac{6M_{ij}}{\beta\hbar^2} \right)} du \quad (2)$$

where $M_{ij} = m_i m_j (m_i + m_j)^{-1}$ is the reduced mass of the interacting particles, $\beta = (k_B T)^{-1}$ with k_B the Boltzmann constant, u the path involved and $V(r_{ij})$ is the classical interaction potential between a pair of particles. The analytical integration of this equation is practically infeasible. To overcome this difficulty, the potential $V(r_{ij})$ is expanded in a Taylor series around r up to the 4th order. After integration we obtain³⁸:

$$V_{FH}(r_{ij}) = V(r_{ij}) + \frac{\beta\hbar^2}{24M_{ij}} \left(\frac{2}{r_{ij}} \frac{\partial V(r_{ij})}{\partial r_{ij}} + \frac{\partial^2 V(r_{ij})}{\partial r_{ij}^2} \right) + \frac{1}{2} \left(\frac{\beta\hbar^2}{24M_{ij}} \right)^2 \left(\frac{4}{r_{ij}} \frac{\partial^3 V(r_{ij})}{\partial r_{ij}^3} + \frac{\partial^4 V(r_{ij})}{\partial r_{ij}^4} \right) \quad (3)$$

For a classical Lennard-Jones potential $V(r_{ij})$, Eq. (2) becomes:

$$V_{LJ-FH}(r_{ij}) = 4\epsilon_{ij} \left(\frac{\sigma_{ij}^{12}}{r_{ij}^{12}} - \frac{\sigma_{ij}^6}{r_{ij}^6} + \frac{\beta\hbar^2}{24M_{ij}} \left(132 \frac{\sigma_{ij}^{12}}{r_{ij}^{14}} - 30 \frac{\sigma_{ij}^6}{r_{ij}^8} \right) + \frac{1}{2} \left(\frac{\beta\hbar^2}{24M_{ij}} \right)^2 \left(24024 \frac{\sigma_{ij}^{12}}{r_{ij}^{16}} - 1680 \frac{\sigma_{ij}^6}{r_{ij}^{10}} \right) \right) \quad (4)$$

The calculation of Feynman-Hibbs approach is implemented in the DL_MONTE Monte Carlo simulation package only to the 2nd order. It has been shown that the expression given in Eq.(4) (4th order) is more accurate for confined fluids at cryogenic temperature²². For this reason we incorporated this correction in the DL_MONTE code.

For single gas adsorption, the insertion-deletion movements correspond to 50 % of the total moves and other movements correspond to translations. For mixtures, only 45 % insertion–deletion moves were used, the remaining 5 % being converted to identity-swap moves to accelerate the equilibration phase. Between 5 to 15 million Monte Carlo cycles, depending on the pressure, were necessary for reaching the equilibrium. And for data analysis 3 million simulation cycles were carried out. For each adsorption isotherm a total of 21 simulations were performed.

Zeolites and hydrogen isotopes

GCMC simulations were performed on pure silica FAU, MFI and CHA zeolites. Their structure was considered as rigid. Cell parameters and atomic positions were those given in the database of zeolite structures of the International Zeolite Association (IZA). The positions of the atoms inside the unit cell were relaxed by DFT (density functional theory) calculations namely with the VASP package, using the PBE-D3 exchange-correlation functional with dispersion corrections. The cut-off radius, above which the molecular interactions are neglected, was 1.5 nm. The simulation box was built with 8 (2x2x2), 12 (2x2x3) and 27 (3x3x3) unit cells for FAU, MFI and CHA zeolites, respectively.

Hydrogen isotopes were represented by a single sphere model with only one van der Waals interaction site per molecule and without electrical charge.

Force fields for adsorbate-adsorbate and adsorbate-adsorbent interactions

Two force fields given in the literature were used to describe the adsorbate - adsorbent (H_2 - zeolite) and adsorbate - adsorbate (H_2 - H_2) interactions. The first one was proposed by Deeg et al.³⁹. It allowed a satisfactory modeling of the adsorption isotherm of hydrogen in all-silica ITQ-27 and MFI zeolites at 77 K. The second one, taken from Pantatosaki et al.²⁴, gave a good prediction of adsorption isotherms of H_2 and D_2 in NaX zeolite at 77 K. Note that this latter force field uses only the H_2 - O potential to describe the adsorbate - adsorbent interactions. Then, we have developed a new force field, called here ASP (Adsorption sur Solides Poreux), by using the potential of Buch⁴⁰ for the H_2 - H_2 interactions and by adjusting the Lennard-Jones parameters of the H_2 -O and H_2 -Si potentials on our experimental data obtained below 77 K. In table 2 are given the parameters for the potential mentioned above.

Accuracy evaluation of the simulations

The deviation between the molecular simulations and the experiments is assessed by mean of the relative average deviation (RAD) defined by:

$$\%RAD = \frac{100}{N} \sum_N \left| \frac{X_{exp,i} - X_{sim,i}}{X_{exp,i}} \right| \quad (5)$$

with $X_{exp,i}$ and $X_{sim,i}$ the values (adsorbed amount N^a or adsorption selectivity α_{D_2/H_2}) measured and simulated in the same conditions. N is the number of computed values. We consider that values of RAD higher than 30 % are not acceptable. This upper limit is based on our experience in the field. We have performed a number of selectivity predictions from single adsorption isotherms by using the Ideal Adsorbed Solution Theory or extended Langmuir model for several binary systems (p-xylene and m-xylene in FAU, linear and branched paraffins in MFI, toluene and mercaptans in FAU, water and formaldehyde in FAU...). The accuracy of the selectivity determination is strongly dependent on the precision at which the adsorption isotherms are measured, simulated by GCMC or described by a classical adsorption model. Our results show that with a RAD above 30 % on single

adsorption isotherm, the predicted adsorption selectivities are too much far from the experimental ones, with average deviation exceeding 100 % in some cases.

Results and discussion

Previous Force fields

Figure 1a shows the adsorption isotherms of H₂ in FAU at 77 K and 47 K simulated with the force fields of Pantatosaki and Deeg (Table 2). The simulations are compared with our experimental data. The potential of Pantatosaki does not allow the prediction of the adsorption isotherms of H₂ since they present a RAD of 82 % and 76 % at 77 and 47 K, respectively. This force field does not take into account the H₂ – Si interactions, which can explain in part the observed discrepancy. Similar results were obtained for D₂. An enhanced agreement was obtained by using the force field proposed by Deeg. However, the relative average deviations are still high (RAD of 42 % and 30 % at 77 K and 47 K, respectively). The relative deviations are particularly large at low pressure ($P < 10^4$ Pa) where the GCMC simulations underestimate the adsorbed amounts but the fitting is better above this pressure. The difference could be attributed to the fact that our FAU zeolite is not completely siliceous since few sodium cations remain in the structure. Moreover, the dealumination treatment used to elaborate this material has created a few mesopores which can have hydroxyl groups on their surface. Cations and hydroxyl groups are known to be strong adsorption sites for hydrogen isotopes¹⁸.

For the MFI and CHA zeolite structures, the force field of Pantatosaki does not accurately describe the adsorption of hydrogen isotopes (RAD > 80 % at 77 K). This is illustrated in Figure 1b for the adsorption of H₂ in CHA at 47 K (RAD > 42 %). The force field of Deeg

can correctly predict the adsorption of H₂ and D₂ in MFI zeolite between 77 (RAD < 23 %) and 47 K (RAD < 11 %). For CHA zeolite, it gives also reasonable predictions at 77 K (RAD = 31 %) but overestimates the adsorbed amounts at lower temperature when the pressure increases. Moreover, it does not reproduce the step in the adsorption isotherm, which appears at 47 K above 100 Pa despite a RAD of 27 % (Figure 1b).

These results show that the force fields described in the literature should be used with precaution. Notice that they have been validated with experiments performed essentially at 77 K or above and only for few zeolitic structures. Their use for lower temperatures and other zeolitic structures requires to be validated by experimental data at the same conditions. Henceforth, the transferability of these force fields is questionable. This state of the art led us to develop a new force field to predict the adsorption and coadsorption of hydrogen isotopes in pure silica zeolites below 77 K.

New force field ASP

In our force field, called ASP, the H₂ – H₂ interactions are described with the L-J potential of Buch⁴⁰. As can be seen in figure 2, this potential correctly describes the bulk fluid properties (density versus fugacity) of hydrogen between 40 K and 200 K, at the conditions that the Feynman-Hibbs corrections are used. The L-J parameters of potentials for the H₂ – O and H₂ – Si interactions have been adjusted on the adsorption experimental data of hydrogen on the silica MFI zeolite (Silicalite-1) measured at 65 K and 77 K (Table 2). We have chosen this zeolite because it is free of defects as hydroxyl groups or mesopores and these temperatures rather than 47 K because they are better controlled with our He cryocooler. Adsorption measurements at these temperatures are therefore more accurate. Figure 3a shows the best fitting of the adsorption isotherm of H₂ in silica MFI zeolite at 65 K and 77 K obtained by GCMC after adjustment of the ASP force field (Table 2). The figure shows a remarkable

agreement with experiments with $\text{RAD} = 1\%$ at 65 K, and 4% at 77 K. Moreover, the adsorption of D_2 is nicely reproduced ($\text{RAD} < 7\%$) and indicates that the Feynman-Hibbs approach expanded to the 4th order reproduces coherently the differences between H_2 and D_2 at cryogenic temperature. In Figure 3b, we can see that the prediction is less accurate at 47 K, notably at high pressure, nonetheless it is acceptable with a RAD around 10% . As can be verified in Figure 4, when the new force field is applied to other zeolites such as FAU or CHA, the potential gives acceptable predictions. For silica FAU, the RAD values lie however between 20% and 30% according to the temperature. This could be due to the presence of residual cations in our FAU sample as discussed above. For silica CHA, it is noticeable that the steps observed at 47 K with the adsorption H_2 and D_2 are well reproduced. RAD values are lower than 15% independently of the temperature. These results allow us to confidently say that we have to our disposal a force field reproducing the single adsorption of H_2 and D_2 below 77 K in high silica zeolites of various structures (FAU, MFI, CHA) with a good accuracy. Hence, we can use this potential for the prediction of coadsorption equilibria of hydrogen isotopes.

Adsorption selectivities

The coadsorption isotherms and the adsorption selectivities of D_2 with respect to H_2 have been simulated with the ASP force field for a mixture containing 75% of H_2 and for pressure ranging from 10 to 10^5 Pa. Results obtained with FAU, MFI and CHA zeolites at 47 and 77 K and for different loadings are compared with experimental data in Figure 5. The simulations obtained for silica MFI at 77 K are in very good agreement with experimental data, they present RAD values of 10% . The ASP force field gives also satisfactory predictions of selectivity for silica CHA with RAD of 19 and 10% at 77 and 47 K, respectively. The simulations of the adsorbed amounts are however less accurate (RAD around 30%). The

increase of the selectivity observed at 47 K above 18 molec.uc⁻¹ is well reproduced. In contrast, the agreement between experiments and simulation for the silica FAU zeolite have a RAD of 38 %. Here again, the impossibility to obtain good prediction with this type of silica zeolite could be due to the presence of defects in our sample.

Singular behavior of silica CHA zeolite

Among the three zeolites studied in this work, the silica CHA zeolite shows a particular behavior with a step on the single adsorption isotherm appearing at 47 K (Figure 4b). Notice that the step is more pronounced with H₂ than with D₂. The step appears at different pressures, 15 000 Pa for H₂ and 1 000 Pa for D₂, but at the same filling of ~ 18 molec.uc⁻¹, from GCMC simulations. Worth noticing that the adsorption selectivity of D₂ towards H₂ sharply increases from the same filling, as shown on figure 5. In a recent communication²⁹, we have shown, by analyzing the density profiles of molecules adsorbed in the cages calculated by GCMC, that this step is the result of a molecular rearrangement of the adsorbed phase induced by confinement effects. Below 18 molec.uc⁻¹, the H₂ and D₂ molecules are adsorbed in the middle of the cages with a low selectivity (i.e., in similar proportion as in the gas phase). Above this filling, molecules are also adsorbed on a second site located in the octagonal window separating two cages with a selectivity largely in favor of D₂. This result may suggest that the difference in adsorbate-adsorbent interactions between H₂ and D₂ is more important on this second adsorption site. For corroborating this hypothesis, here we present a thermodynamic interpretation of our GCMC simulations.

For the adsorption of a single component, the equality of chemical potentials of adsorbed and gas phases at equilibrium leads to the relation:

$$\ln \left(\frac{P}{P^0} \right)_{N^a} = \frac{\Delta H^a}{R} \frac{1}{T} - \frac{\Delta S^a}{R} \quad (6)$$

where ΔH^a and ΔS^a are the molar adsorption enthalpy and entropy at the filling N^a . They are considered as independent on the temperature.

The adsorption enthalpy can be calculated at a given filling from the GCMC simulations by means of the relation:

$$\Delta H^a = \frac{\langle EN \rangle - \langle E \rangle \langle N \rangle}{\langle N^2 \rangle - \langle N \rangle^2} - k_B T \quad (7)$$

with N the number of particles, E the configurational energy and k_B the Boltzmann constant.

This adsorption enthalpy is the opposite of the well-known isosteric heat of adsorption ($\Delta H^a = -Q_{st}$). If the value of ΔH^a is known, the adsorption entropy can be easily calculated at different filling by means of the equation (6) and the adsorption isotherm $N^a = f(P)_T$.

The adsorption enthalpies and entropies for pure H₂ and D₂ in silica FAU, MFI and CHA are given in Figure 6 as a function of filling at 47 K.

For CHA zeolite, the adsorption enthalpies extrapolated at zero filling are slightly lower for D₂ than for H₂ (-5.7 against -5.5 kJ.mol⁻¹) indicating that the adsorbate-adsorbent interactions are stronger with D₂. This is along with the quantum sieving theory, which states that the heavier isotopes are more strongly adsorbed. The values of adsorption enthalpies are of the same order of magnitude as those determined from the experimental adsorption isotherms which lies between -5 and -6 kJ.mol⁻¹. As filling increases, the molecules are adsorbed in the middle of CHA cages. For H₂ as for D₂, the adsorption enthalpy decreases continuously because of the interactions between adsorbed molecules which are more and more confined. At a filling of 18 molec.uc⁻¹, the level of confinement is so important that molecules have to be adsorbed on another site near the octagonal window 8MR separating two cages. At this filling, a sharp increase of 1 kJ.mol⁻¹ (around 20 %) of the adsorption enthalpy is observed with H₂ while D₂ exhibits a plateau. After this jump, the adsorption enthalpy decreases with the same slope as before the jump. This suggests that the adsorbate-adsorbate interactions increase in the same way before and after the step. From these results we can consider that the

jump in the adsorption enthalpy curve is due to the adsorption of H₂ with more repulsive adsorbate-adsorbent interactions than with D₂. This explains why the adsorption selectivity of D₂ towards H₂ increases after 18 molec.uc⁻¹. The increase of D₂/H₂ selectivity occurs when the molecules are adsorbed near the octagonal windows. This is in agreement with the quantum sieving theory established by Beenakker² which states that the selectivity increases as the pore diameter decreases. Below 18 molec.uc⁻¹, the molecules are adsorbed in the middle of CHA cages of 0.74 nm diameter while above this filling they are adsorbed near the 8MR windows of 0.37 nm diameter.

In figure 6 are also reported the evolution of adsorption entropies of hydrogen isotopes with filling and similar behaviors are observed with H₂ and D₂. The adsorption entropies continuously decrease in the same way along the filling. We just observe with H₂ a small jump of entropy at 18 molec.uc⁻¹, like for the enthalpy. This jump of both entropy and enthalpy clearly indicates that the step on the adsorption isotherm associated with an increase of D₂/H₂ selectivity is entropy driven, in agreement with a molecular rearrangement of the adsorbed phase. This conclusion is, however, less obvious for D₂ since no increase of entropy is observed. Notice that the adsorption entropies decrease down to values largely below to the deposition entropies. This indicates that molecules adsorbed in the CHA cages are extremely confined. Clearly, they are in a physical state that is more organized than in a compressed gas or in a liquid as it is currently admitted, but more like a solid phase.

Comparison of FAU, MFI and CHA silica zeolites

Among the three silica zeolites studied in this work, the silica CHA appears as the most efficient adsorbent for the separation of H₂ and D₂ by quantum sieving. This is the material which exhibits the best adsorption selectivity in favor of D₂ at 47 K and high filling (Figure 5). Figure 6 reports the comparison of adsorption enthalpies and entropies of H₂ and D₂ in the

three silica zeolites. First, it can be noticed that the adsorption enthalpies are lower for D₂ than for H₂, whatever the zeolites. As mentioned above, this is in agreement with the quantum sieving theory. Second, for each zeolite at low filling the adsorption entropies of H₂ and D₂ are identical, indicating that the confinements of the two isotopes are similar. As filling increases, adsorption entropy decreases more for H₂ than for D₂, in particular with FAU and MFI. As the presence of other molecules reduces the available pore space, H₂ is more confined than D₂ because its effective kinetic diameter is greater at cryogenic temperatures. This is the consequence of the quantum effect that is applied in the simulation through the Feynman-Hibbs correction of the interaction potential.

Silica FAU presents the highest adsorption enthalpies and entropies. This is also the adsorbent which has the largest cages (1.1 nm) and consequently the greatest adsorption capacity. Adsorbate-adsorbent interactions are relatively weak, and confinement is moderate ($\Delta S^a > \Delta S_{deposition}$). Its adsorption selectivity for D₂ is low whatever the filling is (about 1.5).

With cylindrical channels of smaller diameter (0.56 nm), the MFI zeolite presents lower adsorption enthalpies and entropies. Adsorbate-adsorbent interactions are stronger, and the confinement degree is more important than in FAU. According to the quantum sieving theory, this zeolite should be more selective for D₂, at least at low filling where the theory is valid. Surprisingly, the selectivity is the same as for FAU (Figure 5). Nevertheless, the adsorption selectivity increases with the filling in particular above 20 molec.uc⁻¹, when the confinement becomes important ($\Delta S^a < \Delta S_{deposition}$).

Silica CHA exhibits an intermediate behavior. At low filling, the molecules are adsorbed in the middle of cages. The adsorption enthalpy lies between those of FAU and MFI, but the adsorption entropy is slightly lower than for MFI. The adsorbate-adsorbent interactions are weaker than in MFI but the confinement is more important despite the fact that the molecules are adsorbed in larger pores (0.74 nm diameter). The adsorption selectivity is the same as for

the other two zeolites. As the filling increases, the confinement becomes so important that a molecular rearrangement takes place, and the selectivity becomes in favor of D₂, as explained above. Thus, despite the fact that these three zeolites have the same surface chemical features, they exhibit a different behavior from the energetic point of view. These results show that the quantum sieving does not depend only on the pore diameter. The shape of pores is also a parameter which can influence the separation especially at high filling when confinement effects are enhanced.

Estimation of the size of H₂ and D₂ molecules at different temperatures

Given the correct description of hydrogen isotopes adsorption in silica zeolites by the developed ASP potential, we used it to estimate the size of H₂ and D₂ molecules at different temperatures. This information is crucial for hydrogen isotope separation, however the size estimation currently used in some works raises serious questions. For instance, Cao et al.⁴¹ propose to use the de Broglie wavelength of molecules (λ) as a measure of their “swelling” which is added to the “hard core” to obtain the molecular sizes at different temperatures. The physical basis of this approach is not clear, since the de Broglie wavelength does not characterize any “swelling”, but the wave-like behavior of a quantum particle⁴². In this sense the value of the de Broglie wavelength of H₂ or D₂ at low temperature was applied to the analysis of quantum sieving in the work of Beenakker et al.². Under cryogenic conditions λ_{H_2} and λ_{D_2} are comparable with the difference between the pore diameter and the molecular size, this difference is used as a criterion (of necessity) to take into account quantum effects. This approach by no means justifies the use of the de Broglie wavelength as a measure of molecular “swelling” under low temperature.

Here, we propose to estimate the molecular size of H₂ and D₂ by using the shape of LJ-FH potential. Indeed, in LJ potential the distance corresponding to the minimum in the potential

curve (σ_0) corresponds to the equilibrium separation between two molecules and can therefore be used as estimation of their size. In the case of LJ potential it can be shown that $\sigma_0 = 2^{1/6}\sigma$, but for the combined LJ-FH potential no simple expression can be obtained. Nevertheless, the LJ-FH potential has a minimum whose position depends on temperature and on the molecular mass, as illustrated by the data calculated at 30 K (Figure 7). The distance corresponding to the minimum can be considered as the size of D₂ or H₂ molecules. Obviously, the molecular sizes obtained in this way should not be considered as some absolute values since they are calculated in the particular framework used in this study (spherical D₂ and H₂ molecules interacting via LJ-FH potential). Despite this limitation, we consider that the obtained values can be used as a physically sound estimation of the temperature effect on the size of D₂ and H₂.

The values of H₂ and D₂ sizes at different temperatures obtained using the described approach are presented in Table 3 and in Figure 8. As expected, the size of both D₂ and H₂ increases by lowering the temperature, but not to the same extent. This effect results in a significant increase of the size difference from 0.0056 nm at 100 K to 0.0148 nm at 40 K. Moreover, this difference appears to vary linearly with the inverse of the temperature (Figure 8). It is instructive to compare the calculated size differences with the same parameter for other couples of molecules being separated by adsorption on porous solids. According to the classification proposed by Adil et al.⁴³, D₂/H₂ separation would be of the highest (3rd) level of complexity concerning the separation of molecules with size difference of 0.01 – 0.025 nm. In the same class we find N₂/CH₄ or N₂/O₂ couples whose size difference (~ 0.015 nm) is similar to that calculated for D₂ and H₂ below 40 K. Despite the small size difference, N₂/CH₄ or N₂/O₂ couples can be separated by molecular sieving, i.e., using a material adsorbing only one component. This result suggests that the same process can be realized for hydrogen isotopes by using adsorbents with the appropriate pore size.

Conclusion

Our adsorption experiments of H₂ and D₂ in FAU, MFI and CHA silica zeolites below 77 K were used to test the force fields proposed in the literature. These force fields have been adjusted mainly for measurements performed at 77 K and because of the lack of experimental data at lower cryogenic temperature. We clearly showed that they do not predict accurately the adsorption equilibria below 77 K. We propose a new force field adjusted with data obtained at 65 K with high silica MFI zeolite. This force field, named ASP, is able to predict the adsorption isotherms at other temperatures (40 – 100 K) and to reproduce with high accuracy the D₂/H₂ adsorption selectivities. A particularity of this force field concerns its transferability to other silica zeolites having different structures, namely: FAU and CHA zeolites. Moreover, it nicely reproduces the step observed on the adsorption isotherm with CHA at 47 K. This step is concomitant with a sharp increase of the adsorption selectivity towards D₂ observed experimentally at 18 molec.uc⁻¹ which is well reproduced with the proposed potential. The thermodynamical analysis of our GCMC data confirms that the particular behavior of CHA is the results of a molecular rearrangement of the adsorbed phase induced by confinement. A second adsorption site appears where the adsorbate-adsorbent interactions are weaker with H₂ than with D₂.

The three silica zeolites have the same surface chemical properties, but different pore structures. Our results show that the quantum sieving is not only dependent on the pore diameter, but it is also influenced by the pore geometry. According to the pore shape, new adsorption sites can appear due to molecular rearrangement induced by confinement. These

sites are more or less selective, as shown with CHA. This particular phenomenon explains why CHA is more efficient than FAU and MFI zeolites for the separation of H₂ and D₂ by quantum sieving.

We dispose now of an efficient force field to study by GCMC simulation the separation of hydrogen isotopes by quantum sieving in pure silica zeolites. This force field is a useful tool to perform a screening of zeolites in order to identify, from GCMC simulations, which adsorbent presents the best selectivity. This will permit to avoid fastidious coadsorption experiments at cryogenic temperature which are very time consuming. It allows also to study the adsorption of tritiated radioactive isotopes (T₂, HT, DT...) which cannot be manipulated in conventional laboratories. Our results show that the CHA zeolite is a promising adsorbent for hydrogen isotopes separation by quantum sieving. Therefore, it could be interesting to use our force field to simulate the adsorption of hydrogen isotopes on other zeolitic structures having pore diameter below 0.4 nm, i.e. pores formed with 8-membered oxygen ring (8MR) as in CHA. Among the 252 zeolite structures listed in the database of the International Zeolite Association, some structures as LTA, RWR, CDO, RRO, TON, NSI or ITW have 8MR pore windows and can be synthesized in the pure silica form²⁰. It could be relevant to test these structures in particular at very low temperature in order to know if the molecular rearrangement favorable to the adsorption of deuterium could be observed for these zeolites as it was observed for CHA.

In order to increase the accuracy of our GCMC predictions in these high silica zeolites, more efforts have to be done to describe the interactions between the zeolites and the hydrogen. They must be more realistic by taking into account: (i) the zeolite structure at cryogenic temperature (cell parameters) in particular its flexibility with the temperature and the loading (particularly with zeolite like CHA showing a negative thermal expansion), (ii) the hydrogen molecules which should be described by a more realistic model like dumbbell with partial

electrical charges, (iii) the electrostatic interactions between adsorbate and adsorbent, since the hydrogen isotopes can be polarized by the strong electrical field present in the silica nanopores.

Acknowledgments

Calculations were performed using the resources of DNUM CCUB, the computing center of Université de Bourgogne. The authors thank J. Patarin from IS2M laboratory (Mulhouse, France) who kindly provided the sample of pure silica chabazite used in our experiments. B. Radola thanks the CEA for its financial support.

Conflicts of interest

They are no conflicts to declare

References

1. M. Glugla, A. Busigin, L. Dörr, R. Haange, T. Hayashi, O. Kveton, R. Lässer, D. K. Murdoch, M. Nishi, R. D. Penzhorn and H. Yoshida, *Fusion Engineering and Design*, 2001, **58-59**, 349-353.
2. J. J. M. Beenakker, V. D. Borman and S. Y. Krylov, *Chemical Physics Letters*, 1995, **232**, 379-382.
3. D. M. Ruthven, *Principles of adsorption & adsorption processes*, 1985.
4. J. Y. Kim, H. Oh and H. R. Moon, *Advanced Materials*, 2019, **31**, 1805293.
5. Y. Wang and S. K. Bhatia, *The Journal of Physical Chemistry C*, 2009, **113**, 14953-14962.

6. Y. Wang and S. K. Bhatia, *Molecular Simulation*, 2009, **35**, 162-171.
7. S. R. Challa, D. S. Sholl and J. K. Johnson, *Physical Review B*, 2001, **63**, 245419.
8. X. Zhao, S. Villar-Rodil, A. J. Fletcher and K. M. Thomas, *The Journal of Physical Chemistry B*, 2006, **110**, 9947-9955.
9. A. Gotzias, G. Charalambopoulou, A. Ampoumogli, I. Krkljus, M. Hirscher and T. Steriotis, *Adsorption*, 2013, **19**, 373-379.
10. H. Oh, S. B. Kalidindi, Y. Um, S. Bureekaew, R. Schmid, R. A. Fischer and M. Hirscher, *Angewandte Chemie International Edition*, 2013, **52**, 13219-13222.
11. J. Y. Kim, L. Zhang, R. Balderas-Xicohténcatl, J. Park, M. Hirscher, H. R. Moon and H. Oh, *Journal of the American Chemical Society*, 2017, **139**, 17743-17746.
12. L. Zhang, S. Jee, J. Park, M. Jung, D. Wallacher, A. Franz, W. Lee, M. Yoon, K. Choi, M. Hirscher and H. Oh, *Journal of the American Chemical Society*, 2019, **141**, 19850-19858.
13. I. Bezverkhyy, Q. Pujol, C. Dirand, F. Herbst, M. Macaud and J.-P. Bellat, *Microporous and Mesoporous Materials*, 2020, **302**, 110217.
14. A. J. W. Physick, D. J. Wales, S. H. R. Owens, J. Shang, P. A. Webley, T. J. Mays and V. P. Ting, *Chemical Engineering Journal*, 2016, **288**, 161-168.
15. X.-Z. Chu, Z.-P. Cheng, X.-X. Xiang, J.-M. Xu, Y.-J. Zhao, W.-G. Zhang, J.-S. Lv, Y.-P. Zhou, L. Zhou, D.-K. Moon and C.-H. Lee, *International Journal of Hydrogen Energy*, 2014, **39**, 4437-4446.
16. K. Kotoh, T. Nishikawa and Y. Kashio, *Journal of Nuclear Science and Technology*, 2002, **39**, 435-441.
17. K. Kotoh, S. Takashima and Y. Nakamura, *Fusion Engineering and Design*, 2009, **84**, 1108-1112.
18. M. Giraudet, I. Bezverkhyy, G. Weber, C. Dirand, M. Macaud and J.-P. Bellat, *Microporous and Mesoporous Materials*, 2018, **270**, 211-219.
19. J. Perez-Carbajo, J. B. Parra, C. O. Ania, P. J. Merkling and S. Calero, *ACS Applied Materials & Interfaces*, 2019, **11**, 18833-18840.
20. Y. G. Bushuev and G. Sastre, *The Journal of Physical Chemistry C*, 2010, **114**, 19157-19168.
21. A. H. Fuchs and A. K. Cheetham, *The Journal of Physical Chemistry B*, 2001, **105**, 7375-7383.
22. A. V. A. Kumar, H. Jobic and S. K. Bhatia, *The Journal of Physical Chemistry B*, 2006, **110**, 1666-16671.

23. A. V. A. Kumar, H. Jobic and S. K. Bhatia, *Adsorption*, 2007, **13**, 501-508.
24. E. Pantatosaki, G. K. Papadopoulos, H. Jobic and D. N. Theodorou, *The Journal of Physical Chemistry B*, 2008, **112**, 11708-11715.
25. P. Kowalczyk, A. P. Terzyk, P. A. Gauden, S. Furmaniak, E. Pantatosaki and G. K. Papadopoulos, *The Journal of Physical Chemistry C*, 2015, **119**, 15373-15380.
26. J. M. Salazar, S. Lectez, C. Gauvin, M. Macaud, J. P. Bellat, G. Weber, I. Bezverkhyy and J. M. Simon, *International Journal of Hydrogen Energy*, 2017, **42**, 13099-13110.
27. J. M. Salazar, M. Badawi, B. Radola, M. Macaud and J. M. Simon, *The Journal of Physical Chemistry C*, 2019, **123**, 23455-23463.
28. A. V. A. Kumar and S. K. Bhatia, *Physical Review Letters*, 2005, **95**, 245901.
29. B. Radola, I. Bezverkhyy, J.-M. Simon, J. M. Salazar, M. Macaud and J.-P. Bellat, *Chemical Communications*, 2020, DOI: 10.1039/D0CC02060E.
30. J. L. Guth, H. Kessler and R. Wey, in *Studies in Surface Science and Catalysis*, eds. Y. Murakami, A. Iijima and J. W. Ward, Elsevier, 1986, vol. 28, pp. 121-128.
31. M.-J. Díaz-Cabañas and P. A. Barrett, *Chemical Communications*, 1998, DOI: 10.1039/A804800B, 1881-1882.
32. G. Gregis, S. Schaefer, J.-B. Sanchez, V. Fierro, F. Berger, I. Bezverkhyy, G. Weber, J.-P. Bellat and A. Celzard, *Materials Chemistry and Physics*, 2017, **192**, 374-382.
33. T. Karbowski, M.-A. Saada, S. Rigolet, A. Ballandras, G. Weber, I. Bezverkhyy, M. Soulard, J. Patarin and J.-P. Bellat, *Physical Chemistry Chemical Physics*, 2010, **12**, 11454-11466.
34. J. A. Purton, J. C. Crabtree and S. C. Parker, *Molecular Simulation*, 2013, **39**, 1240-1252.
35. A. V. Brukhno, J. Grant, T. L. Underwood, K. Stratford, S. C. Parker, J. A. Purton and N. B. Wilding, *Molecular Simulation*, 2019, DOI: 10.1080/08927022.2019.1569760, 1-21.
36. R. P. Feynman and A. R. Hibbs, *Quantum Mechanics and Path Integrals*, 1965.
37. L. M. Sesé, *Molecular Physics*, 1994, **81**, 1297-1312.
38. L. M. Sesé, *Molecular Physics*, 1995, **85**, 931-947.
39. K. S. Deeg, J. J. Gutiérrez-Sevillano, R. Bueno-Pérez, J. B. Parra, C. O. Ania, M. Doblare and S. Calero, *The Journal of Physical Chemistry C*, 2013, **117**, 14374-14380.
40. V. Buch, *The Journal of Chemical Physics*, 1994, **100**, 7610-7629.

41. D. Cao, H. Huang, Y. Lan, X. Chen, Q. Yang, D. Liu, Y. Gong, C. Xiao, C. Zhong and S. Peng, *Journal of Materials Chemistry A*, 2018, **6**, 19954-19959.
42. P. W. Atkins and J. Paula, *Physical Chemistry*, Oxford University Press, New York, 2006.
43. K. Adil, Y. Belmabkhout, R. S. Pillai, A. Cadiou, P. M. Bhatt, A. H. Assen, G. Maurin and M. Eddaoudi, *Chemical Society Reviews*, 2017, **46**, 3402-3430.

Tables

Table 1: Some physical-chemical properties of high silica zeolites (the pore volume is the one accessible to nitrogen at 77 K).

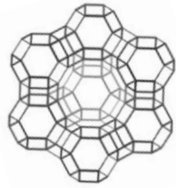
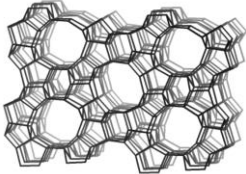
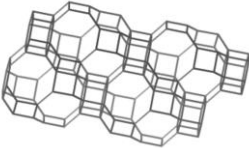
Zeolite	Composition	Structure	Pore volume (cm ³ .g ⁻¹)	Pore diameter (nm)
FAU	Na ₂ [Al ₂ Si ₁₉₀ O ₃₈₄]		0.293	Spherical cages: 1.1 12 MR window: 0.74
MFI	Si ₉₆ O ₁₉₂		0.180	10 MR cylindrical channels: 0.56
CHA	Si ₃₆ O ₇₂		0.250	Ovoid cages: 0.74 8MR window: 0.37

Table 2: Lennard-Jones interaction parameters used to describe the adsorbate-adsorbate and adsorbate-adsorbent interactions. The parameters for D₂ are the same as for H₂.

Interaction	adsorbate - adsorbate		adsorbate - adsorbent			
	H ₂ - H ₂		H ₂ - O		H ₂ - Si	
L-J parameter	σ (nm)	ϵ (K)	σ (nm)	ϵ (K)	σ (nm)	ϵ (K)
Deeg et al. ³⁹	0.2959	36.70	0.2890	66.06	0.1854	28.26
Pantatosaki et al. ²⁴	0.2820	36.50	0.2800	56.00	-	-
ASP	0.2920	38.00	0.3080	47.00	0.2800	39.00

Table 3: Effective size of D₂ and H₂ determined at different temperatures from the FH-LJ potential of interaction.

T (K)	$\sigma_{0(D_2)}$ (nm)	$\sigma_{0(H_2)}$ (nm)	$\sigma_{0(D_2)} - \sigma_{0(H_2)}$ (nm)
100	0.3335	0.3391	0.0056
90	0.3342	0.33403	0.0061
77	0.3352	0.34230	0.0071
70	0.3360	0.3436	0.0076
60	0.3373	0.3460	0.0087
50	0.3391	0.3493	0.0102
40	0.3418	0.3539	0.0121
30	0.3461	0.3609	0.0148

Figures

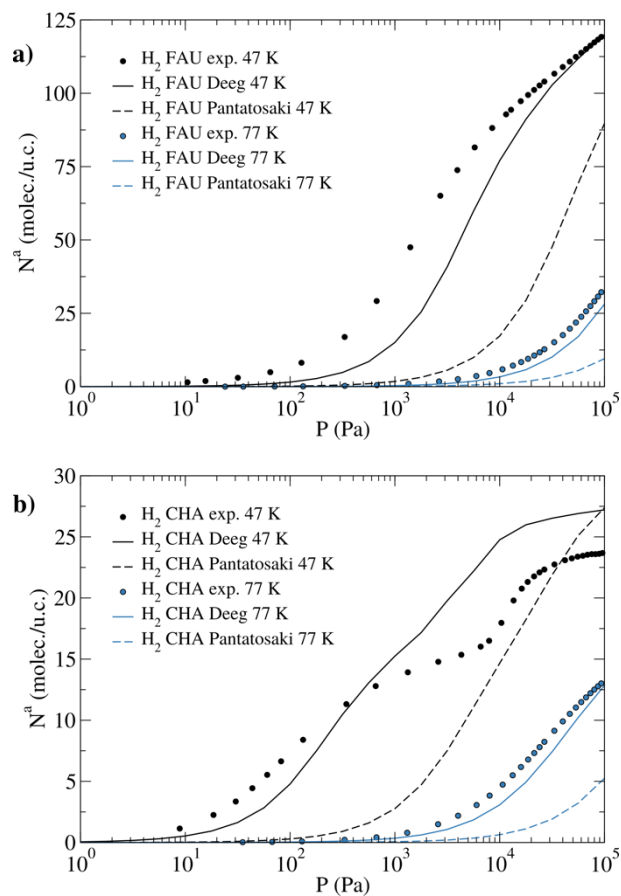


Figure 1: Adsorption isotherms of H₂ in a) silica FAU zeolite and b) silica CHA zeolite at 47 K and 77 K. Full circles: experiments. Dashed lines: GCMC simulations with Pantatosaki's force field. Solid lines: GCMC simulations with Deeg's force field.

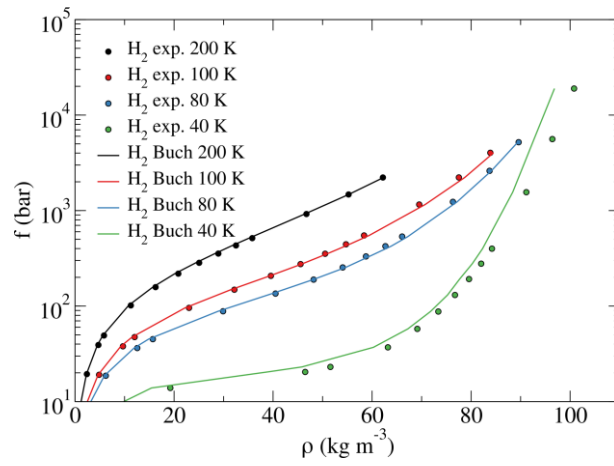


Figure 2: Dependence of density on fugacity for hydrogen fluid at high fugacity and low temperature. Full circles: experimental data taken from Younglove. Solid lines: GCMC simulations using the Buch force field and the 4th order Feynman-Hibbs potential.

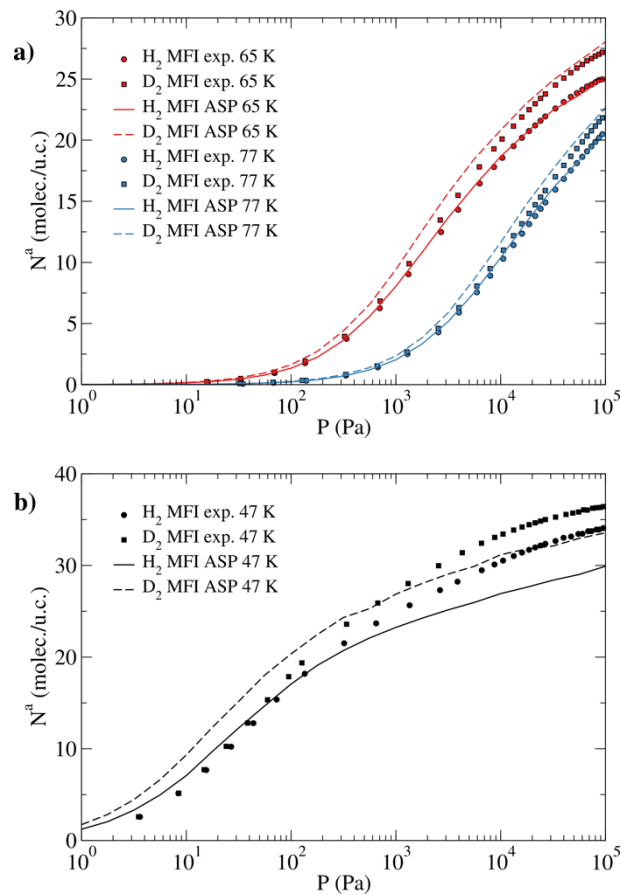


Figure 3: Adsorption isotherms of H_2 and D_2 on silica MFI simulated with the ASP force field: a) $T = 65$ K and 77 K and b) $T = 47$ K. Full circles: experiments. Solid lines: GCMC for H_2 . Dashed lines: GCMC for D_2 .

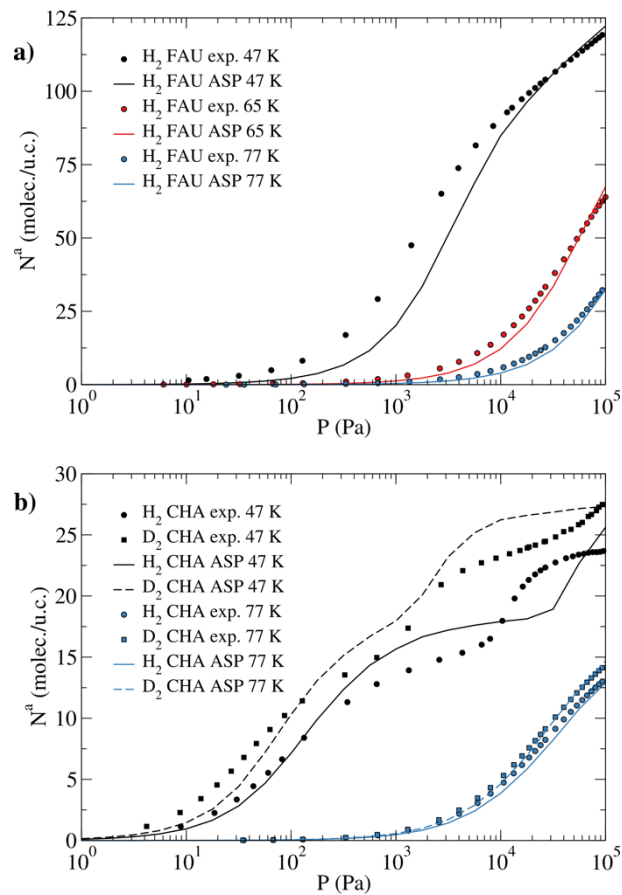


Figure 4: Adsorption isotherms simulated with the ASP force field: a) H_2 in silica FAU at 47 K, 65 K and 77 K and b) H_2 and D_2 in silica CHA at 47 K and 77 K. Full circles: experiments. Solid lines: GCMC for H_2 . Dashed lines: GCMC for D_2 .

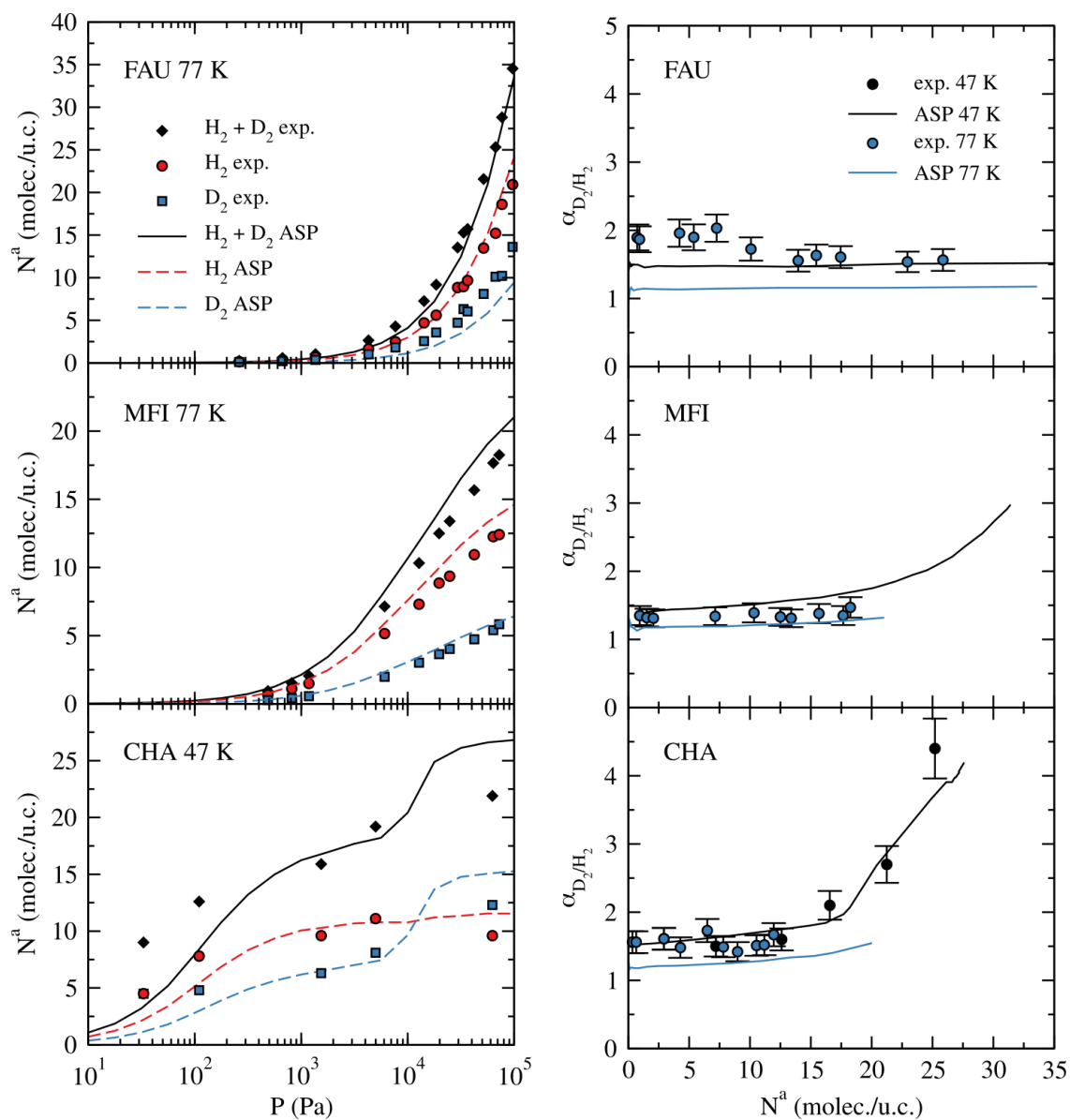


Figure 5: Coadsorption isotherms (left) and adsorption selectivities (right) for a 75% H_2 + 25% D_2 mixture on FAU, MFI and CHA silica zeolites. Symbols: experiments. Solid and dashed lines: GCMC simulations with the ASP force field.

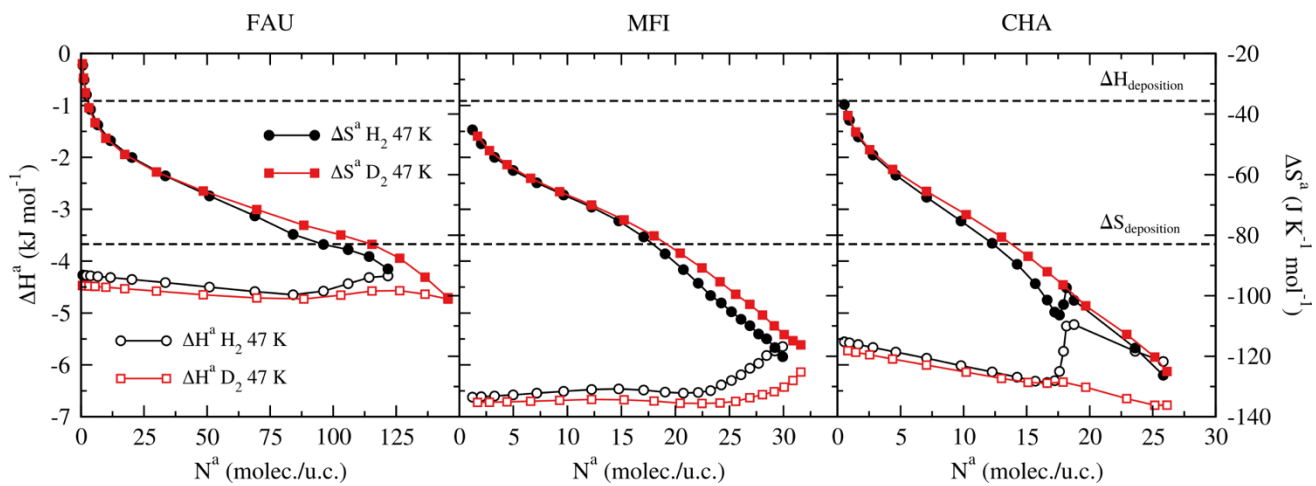


Figure 6: Adsorption enthalpies (open symbols) and entropies (full symbols) of D_2 (squares) and H_2 (circles) in FAU, MFI and CHA silica zeolites, determined from GCMC simulations at 47 K. Dashed lines correspond to the enthalpy and entropy of deposition of H_2 .

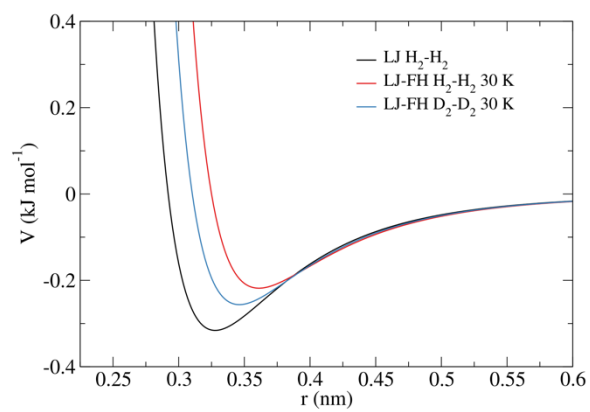


Figure 7: L-J and FH-LJ potentials of interaction for H_2 and D_2 as a function of the distance at 30 K.

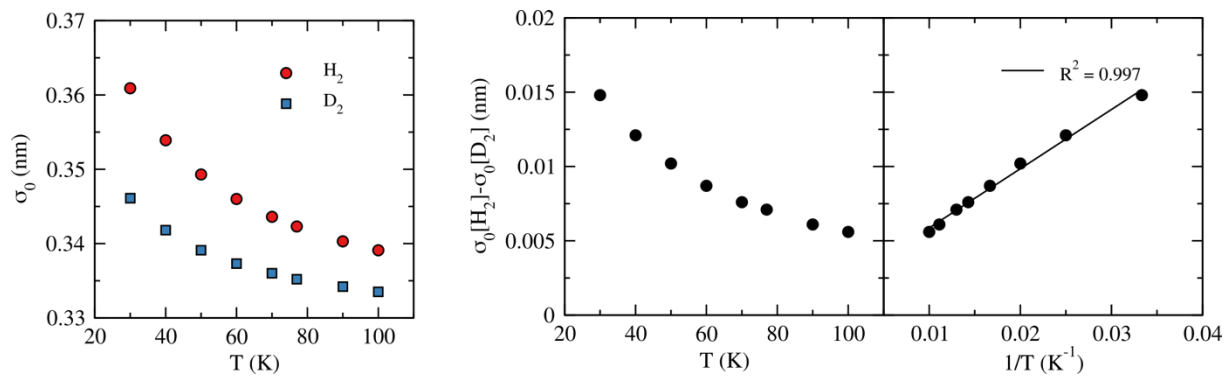


Figure 8: Dependence of the temperature on the effective size of D_2 and H_2 calculated from FH-LJ potential of interaction.